

①



National Defence / Defense nationale



MICRO-RADIOGRAPHY USING AN ELECTRON LINAC SOURCE AND RAM MEMORY CHIP DETECTORS (U)

by

T. Cousins, E.L. Karam and J.R. Brisson

AD-A229 658

DTIC
ELECTE
DEC 04 1990
S E D
CO

DEFENCE RESEARCH ESTABLISHMENT OTTAWA
TECHNICAL NOTE 90-16

Canada

DISTRIBUTION STATEMENT A
Approved for public release
Distribution Unlimited

June 1990
Ottawa



National Défense
 Defence nationale

MICRO-RADIOGRAPHY USING AN ELECTRON LINAC SOURCE AND RAM MEMORY CHIP DETECTORS (U)

by

T. Cousins, E.L. Karam and J.R. Brisson
*Nuclear Effects Section
 Electronics Division*

DTIC
 COPY
 INSPECTION
 6

Accession For	
DTIS GRA&I	<input checked="" type="checkbox"/>
DTIC TAB	<input type="checkbox"/>
Unannounced	<input type="checkbox"/>
Justification	
By _____	
Distribution/	
Availability Codes	
Dist	Avail and/or Special
A-1	

DEFENCE RESEARCH ESTABLISHMENT OTTAWA
 TECHNICAL NOTE 90-16

PCN
 041LS

DISTRIBUTION STATEMENT A
 Approved for public release;
 Distribution Unlimited

June 1990
 Ottawa

ABSTRACT

Radiography using a pulsed electron (LINAC) source and a semiconductor memory chip (RAM) as a detector has been investigated. The responses of commercial SRAMS and DRAMS were examined, with the SRAM proving superior for radiography. A variety of shapes (circular holes, slits, etc.) were radiographed with encouraging results for future work.

RESUME

Une méthode de radiographie utilisant comme source un accélérateur linéaire d'électron à impulsion (LINAC) et utilisant des mémoires à circuits intégrés comme détecteur est étudiée dans ce rapport. La réponse de mémoires statiques et dynamiques (SRAMS et DRAMS) commerciales est examinée, démontrant que les mémoires statiques sont supérieures pour cette application. Plusieurs formes (trous circulaires, fentes, etc.) ont été radiographiées, fournissant des résultats très encourageant.

EXECUTIVE SUMMARY

A radiographic system employing a pulsed electron LINAC as the radiation source and commercially available semiconductor memories (RAMs) as the detector has been investigated. An NMOS SRAM proved markedly superior to an NMOS DRAM for radiography, showing the ability to reproduce a variety of shapes (circular holes, slits, etc.). The exceptional resolution of the system (owing to the extremely small size of individual bits in modern semiconductor memories) may make future development of the system attractive.

TABLE OF CONTENTS

	<u>Page</u>
ABSTRACT/RESUMÉ	iii
EXECUTIVE SUMMARY	v
TABLE OF CONTENTS	vii
LIST OF FIGURES	ix
1.0 INTRODUCTION	1
2.0 THEORY	1
2.1 Advantages of Memory Chips over Photographic Methods	1
2.2 Comparison of the Use of Electrons and Gamma-Rays as Radiographic Sources	2
3.0 EXPERIMENTAL	3
3.1 MS2200 Memory Tester	3
3.2 Irradiation Facility	3
4.0 RESULTS	4
4.1 NEC DRAM	4
4.2 AMD SRAM	5
5.0 CONCLUSIONS	5
6.0 REFERENCES	21

LIST OF FIGURES

	<u>Page</u>
Figure 1:	Physical layout of AMD2167 16k x1 SRAM, along with appropriate dimensions. 6
Figure 2:	Physical layout of NEC μ 41256 256k x1 DRAM, along with appropriate dimensions. 7
Figure 3:	Absorption of 1 MeV electrons in Aluminum. 8
Figure 4:	Comparison of attenuation of 10 MeV electrons and ^{60}Co gamma-rays in Pb and Al. 9
Figure 5:	FCR display showing the transmission pattern of 8 MeV electrons through 1/32" collimator onto NEC DRAM. Note the central pattern caused by direct ionization, and the photocurrent effects along the x and y decoder lines. 10
Figure 6:	FCR display showing transmission pattern of 8 MeV electrons through 1/32" collimator onto the NEC DRAM, aimed directly at the chip centre (intersection of x and y decoder lines). The transmission along the decoder lines masks the collimator image. 11
Figure 7:	The same experimental set up as in Fig. 6, but at a higher dose rate. Note that spreading and decoder line effects render recognition of the direct collimator image impossible. 12
Figure 8(a):	FCR display showing transmission pattern of 8 MeV electrons through 1/32" collimator onto the AMD SRAM, with all bits originally set to '0'. Note the elliptical image due to cell aspect ratio. 13
Figure 8(b):	FCR display showing transmission pattern of 8 MeV electrons through 1/32" collimator onto the AMD SRAM, with all bits originally set to '1'. Clearly this setting is more sensitive than the '0' case. 14
Figure 9:	Same experimental set-up as in Fig. 8(b), but with much higher dose rate and with collimator physically moved. Note that although the elliptical pattern grows, it is still recognizable. 15

Figure 10:	FCR display showing the transmission pattern of 8 MeV electrons through a $(.018 \pm .003)$ inch wide slit arranged diagonally across the AMD SRAM chip. The discontinuity is due to the chip decoder strip.	16
Figure 11:	FCR display showing the transmission pattern of 8 MeV electrons through an "inverted T" (formed by the intersection of three Al plates) onto the AMD SRAM.	17
Figure 12:	FCR display showing the transmission pattern on the AMD SRAM arising for an Al plate shadowing the upper half of the chip.	18
Figure 13:	FCR display showing the transmission pattern on the AMD SRAM arising from an Al plate placed diagonally across the chip. Note that decoder strip and some edge effects are apparent.	19
Figure 14:	FCR display showing the transmission pattern on the AMD SRAM arising from a corner of the Al plate intersecting the beam. The decoder strip effects are apparent.	20

1.0 INTRODUCTION

Radiography is the production of images (pictures) upon a sensitive surface (as of a photographic film) by a form of radiation other than light. The most common type of radiography is, of course, the use of X-rays as the radiation source and photographic film as the imaging material - which has given rise to the colloquialism of 'X-ray' for a wide variety of radiographic techniques.

The choice of incident radiation is not however limited to atomic sources. Neutrons (1) and gamma-rays (2) have been employed and their properties can offer attractive alternatives (particularly when the neutron cross sections are taken into account). Recently the idea of using a semiconductor memory chip as the imaging element has been examined (3) with ^{60}Co gamma-rays being the source of radiation. This concept can be dubbed 'micro-radiography' as it allows imaging on a much smaller scale than film processing.

Recent DREO experiments have examined the response of selected memories to a variety of radiation sources (4). Here the MOSAID MS-2200 memory tester system was used to give a real-time bit-map of the device under test (DUT). During the course of this work it became apparent that high energy electrons produced at a LINAC facility might be used as the radiation source for radiography. The use of electrons, with their different transmission characteristics, may offer some advantages over gamma-rays.

This report briefly examines DREO's early findings of the implications of this type of radiography. No effort has been made here to optimize the system either by choice of memory chip or incident radiation energy spectrum/time domain, or by any signal processing on the irradiation image.

2.0 THEORY

2.1 ADVANTAGES OF MEMORY CHIPS OVER PHOTOGRAPHIC METHODS

The two major advantages of the use of memory chips over photographic methods for radiography are spatial resolution and real time data. The latter should be obvious when considering the necessary time for processing exposed film. The immediacy of the results obtained on the MS2200 system has been previously reported - with the only time delay being that time required to run a computer-controlled test file (~ 1 s). The resolution enhancement will be examined below for the two memory devices used in this work.

The two NMOS memory devices used here were the Advanced Micro Devices AM2167 16kx1 SRAM (AMD) and the Nipon Electric Corporation NEC μ 41256 256k x 1 DRAM (NEC). Both devices were chosen primarily because of the availability of the device descrambling codes were obtained, along with the chip layouts from Semiconductor Insights Inc. (5). These physical layouts appear in figs 1 and 2.

It is from these layouts that an estimation of the pixel size for each device can be calculated - i.e. the physical dimensions of each memory cell. This cell size will be the optimum spatial resolution. Of course, the resolution will not be this good if neighbouring cells interact with one another by charge

transfer or other means. This has been shown to be the case for certain irradiation conditions (4). However it is also clear that by judicious choice of these conditions such unwanted secondary effects can be eliminated.

The calculations yield cell sizes of $34 \mu\text{m} \times 17.5 \mu\text{m}$ ($593 \mu\text{m}^2$) for the AMD SRAM and $6.5 \mu\text{m} \times 12.5 \mu\text{m}$ ($81.3 \mu\text{m}^2$) for the NEC DRAM. Both are considerably smaller than typical photographic limits of around 0.1 mm (6). One should note also that the two chips are not highly integrated by today's standards. For example, increasing to a 1M memory on the same size die would decrease each cell dimension by a factor of two (and of course area by a factor of four). The increase in integration also results in an increased memory overall sensitivity to radiation (7) which for these purposes would indeed be beneficial.

2.2. COMPARISON OF THE USE OF ELECTRONS AND GAMMA RAYS AS RADIOGRAPHIC SOURCES

The essential principal which allows successful radiography is that the incident radiation will be transmitted to the detector in an amount determined by the nature and/or thickness of the absorbing material placed between the source and detector. Thus the concept of radiation transmission is the key to understanding radiography. The transmission of electrons and gamma rays through matter involves very different terminologies - with the concept of range being the key for electrons while attenuation coefficients are the key to understanding gamma rays.

The electron range may be evaluated when one examines the absorption of mono-energetic electrons passing through matter. Fig 3 gives this plot, specifically for 1 MeV electrons into Al (from (8)), but the trend is the same for all () 0.6 MeV) electrons. The ratio first decreases slowly with increasing absorber thickness, then decreases linearly and finally merges into the background intensity. Extrapolation of the linear portion of the curve to zero (as done in the dashed line in the figure) yields the so-called practical range R_p .

A relation between range and electron energy has been long-established (9) as

$$R_p \text{ (g/cm}^2\text{)} = 0.526 E(\text{MeV}) - 0.094 \quad (1)$$

Thus knowledge of the absorber thickness in g/cm^2 (a product of density and thickness in cm) will allow evaluation of the relative intensity distributions for electrons.

The transmission of gamma rays through matter is observed to follow, in general, a simple exponential attenuation given by

$$I(x) = I_0 e^{-\Sigma x} \quad (2)$$

where $I(x)$ - transmitted intensity for absorber thickness x
 I_0 - initial γ ray intensity
 Σ - absorption coefficient (cm^{-1})
 x - absorber thickness

A comparison of the relative attenuations for dense (Pb) and light (Al) materials for both 10 MeV electrons and ^{60}Co gamma rays is presented in fig. 4. Here the values for R_p and Σ are taken from (10).

One advantage of the use of electrons over radiography would be that 100% of the electrons are absorbed for the respective ranges of 1.91 cm in Al and 0.457 cm in Pb, whereas the gamma rays are only attenuated by roughly 15% for both. Thus, ideally smaller changes in absorber thickness should be apparent through electron radiography.

An obvious extension of radiography with lower range particles would be the use of an α particle source. Note that for typical (5 meV) α particles the ranges in Pb and Al would be 16 and 25 μm respectively (9). Add to this the known fact that higher LET particles are extremely efficient at creating single event upsets (SEUs) in memories (11), and the prospects for α radiography may be worthwhile investigating.

An additional factor in favour of LINAC radiography lies in their tunability. For example the Chalk River Nuclear Laboratories PHELA facility (12) has an energy range variable from 8 MeV to 12 MeV, resulting in a 33% variation in electron range. It is also possible to change the incident electron spectrum with the use of (Al) filters.

The above arguments concern absorption of electrons and photons only. Any possible transmission of the secondary particles (photons from electrons; electrons from photons) is ignored. The secondary photons from electron interactions (such as Bremsstrahlung) will constitute a significant portion of the transmitted radiation owing to their range. Their effects on the memory response cannot be ignored.

The intentional use of a full Bremsstrahlung convertor would allow for photon pulse/RAM radiography (although of course the total incident particle dose is likely to drop to about 10%). The versatility of a LINAC in this respect can only add to the attractiveness of the work. This option is not pursued here.

3.0 EXPERIMENTAL

3.1 MS2200 MEMORY TESTER

A block diagram of the MOSAID MS2200 memory tester system appears in fig 5. Briefly the memory tester consists of the main system unit, bit-map display monitor, test head unit and an AT compatible computer. A DREO-built 75 foot cable allows remote hook-up of the DUT to the rest of the system. Under computer control, a memory may be programmed prior to irradiation and then interrogated after to find the location of errors through a fast capture RAM (FCR) - thus allowing 'real time' imaging. A more complete description of the MS2200 may be found elsewhere (4).

3.2 IRRADIATION FACILITY

All experiments reported on here were performed at the MEVEX LINAC facility (13). The facility can produce 2 μ s wide pulses of 8 MeV electrons in either single shot or repetitive mode. The large irradiation area allows great variation in dose rate, using simple $1/r^2$ considerations.

4.0 RESULTS

4.1 NEC DRAM

The figures shown in this section are aimed primarily in establishing the feasibility of a LINAC/DRAM radiography system. Again no attempts have been made to optimize results. Significant improvements with only minor modifications should be possible.

A fundamental requirement of any radiographic system is the capability to differentiate between different thicknesses or densities of materials. An elementary test of this is to attempt the imaging of various shapes - holes, edges, etc. For all the tests reported upon here, the absorbers were aluminum, lead or steel plates with thicknesses greater than the range of 8 MeV electrons.

Figure 5 shows an FCR display from the NEC DRAM with 1/2" steel absorber having a 1/32" diameter hole collimator aimed at the area between the ground and decoder lines. The image is quite sharp, and the elliptical nature is caused by the cell aspect ratio. From the die dimensions (in figure 2) one can directly measure the ellipse x-axis to be (0.037 ± 0.03) inches and the y-axis to be (0.039 ± 0.04) inches. Both are in reasonable agreement with the hole diameter of 0.031 inches. The slightly higher values may easily be explained by some beam spreading between the collimator and memory.

Also evident in fig 5 are bit errors near the ground and decoder lines. Previous DREO work (4) has attributed these errors to photocurrent effects, and these errors generally occur before the direct (ionization) errors. When the collimator is aimed to hit directly at chip centre (the intersection of two lines) the pattern in fig 6 is observed. Here the dose rate error pattern masks the collimator pattern, and the elliptical shape is unrecognizable.

Finally fig 7 shows the effect of too much dose rate on the image. The charge spreading effects from one memory cell to its neighbours cause an enlarging of the elliptical pattern which, coupled with the decoder line effects, makes meaningful radiography meaningless.

Thus this particular DRAM, for a variety of reasons, would appear inappropriate for radiography.

4.2 AMD SRAM

Figs 8(a) and 8(b) show the results from the 1/32" collimator irradiations of the AMD SRAM for all bits set to 'zero' and 'one' respectively. Clearly the 'one' setting proved more sensitive. Again the elliptical effect is caused by differences in bit dimensions. The measured values for the axes yielded $(.038 \pm .03)$ inches in the y-direction, and $(.031 \pm .03)$ inches in the x-direction - both in excellent agreement with the hole diameter. Very little other structure is apparent, save some fringing along the left vertical border. This lack of propagation along decoder lines has been previously observed (4). Fig 9 shows the effect of much higher total dose on the FCR display. The ellipse does grow somewhat - but not nearly as much as for the NEC device.

The promise shown by the AMD chip led to further work. Fig 10 shows the FCR display for a $(.018 \pm .003)$ inch wide slit in an aluminum plate, diagonally across the chip. Note the discontinuity caused by the x-decoder line at the centre of the array (fig 1). The width of the image of the slit is $(.025 \pm .003)$ inches, in reasonable agreement with the actual width.

Fig 11 shows the FCR display of an 'inverted T' formed by the intersection of three Al plates. The 'rounding' of the corner in the left hand side of the FCR is believed real. The influence of the decoder strip is apparent on the right side.

Fig 12 shows the result of an Al plate shadowing the upper half of the chip. As in all plots, the incorrect scramble effects show up. The non-linear edge may or may not reflect the true shape of the plate.

Fig 13 shows the effect of an Al plate placed diagonally across the chip. The decoder strip and edge effects are apparent.

Finally, fig 14 shows an FCR from the corner of an Al plate shadowing the chip. The decoder strip causes the expected distortions. The corner however is clearly visible in the right-hand side.

Radiography with the AMD SRAM was not without problems. Chief among these was the tendency of too high a dose to completely wipe out the entire memory - evidence of either synergistic effects or a large Bremsstrahlung component. However in view of the crude nature of this work, LINAC/SRAM radiography would appear to be a distinct possibility.

5.0 CONCLUSIONS

The work presented here represents an extremely crude attempt to use a LINAC/RAM system for micro-radiography. In view of the fact that no optimization of experimental parameters was attempted, the results clearly demonstrate the validity of such a system. The system may offer some advantages over more conventional radiographic techniques.

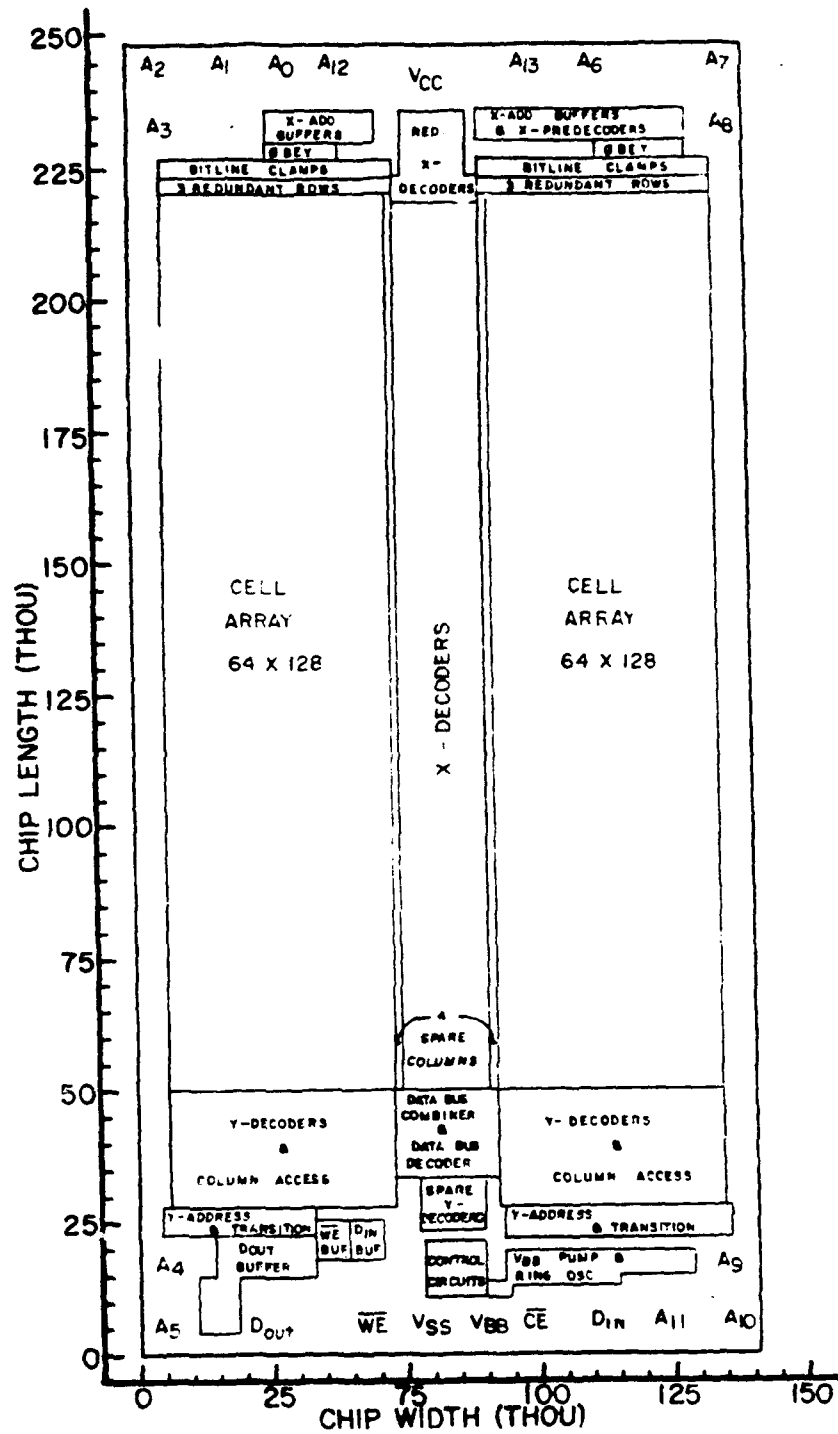


Figure 1: Physical layout of AMD2167 16k x1 SRAM, along with appropriate dimensions.

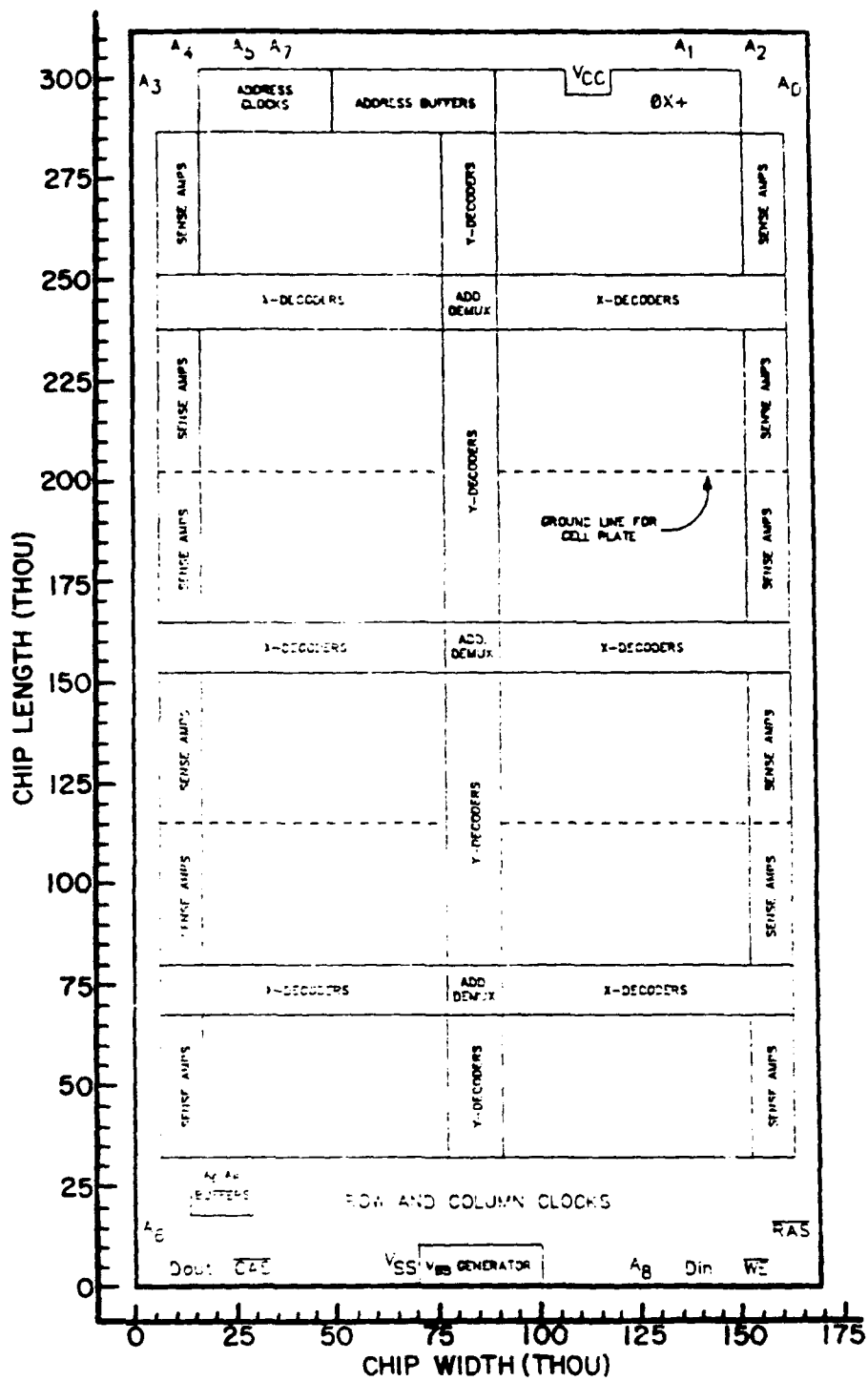


Figure 2: Physical layout of NEC $\mu 41256$ 256k x1 DRAM, along with appropriate dimensions.

1 MeV Electron Absorption in Aluminum

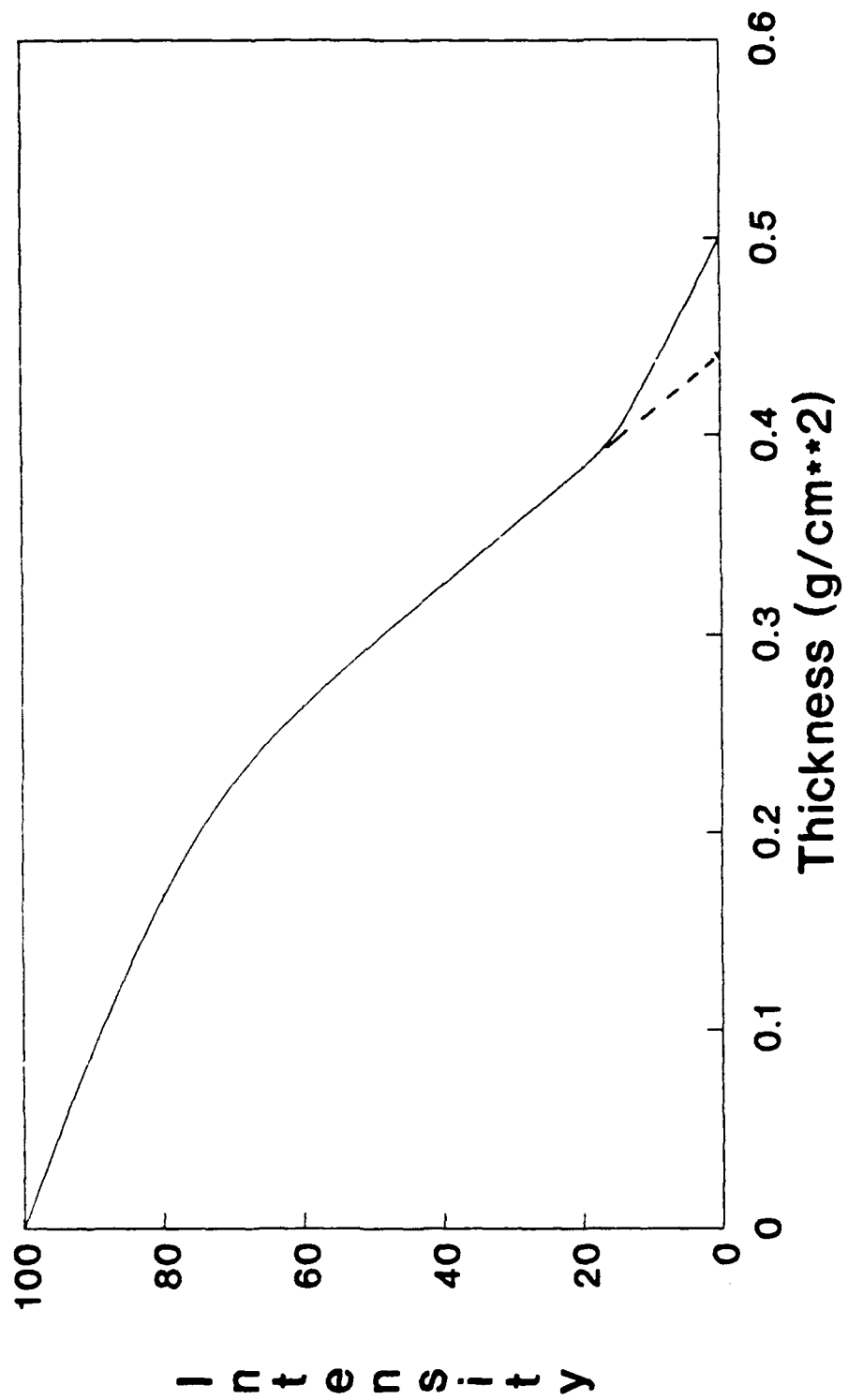


Figure 3: Absorption of 1 MeV electrons in Aluminum.

ATTENUATION OF PHOTONS AND ELECTRONS (COMPARISON IN Al and Pb)

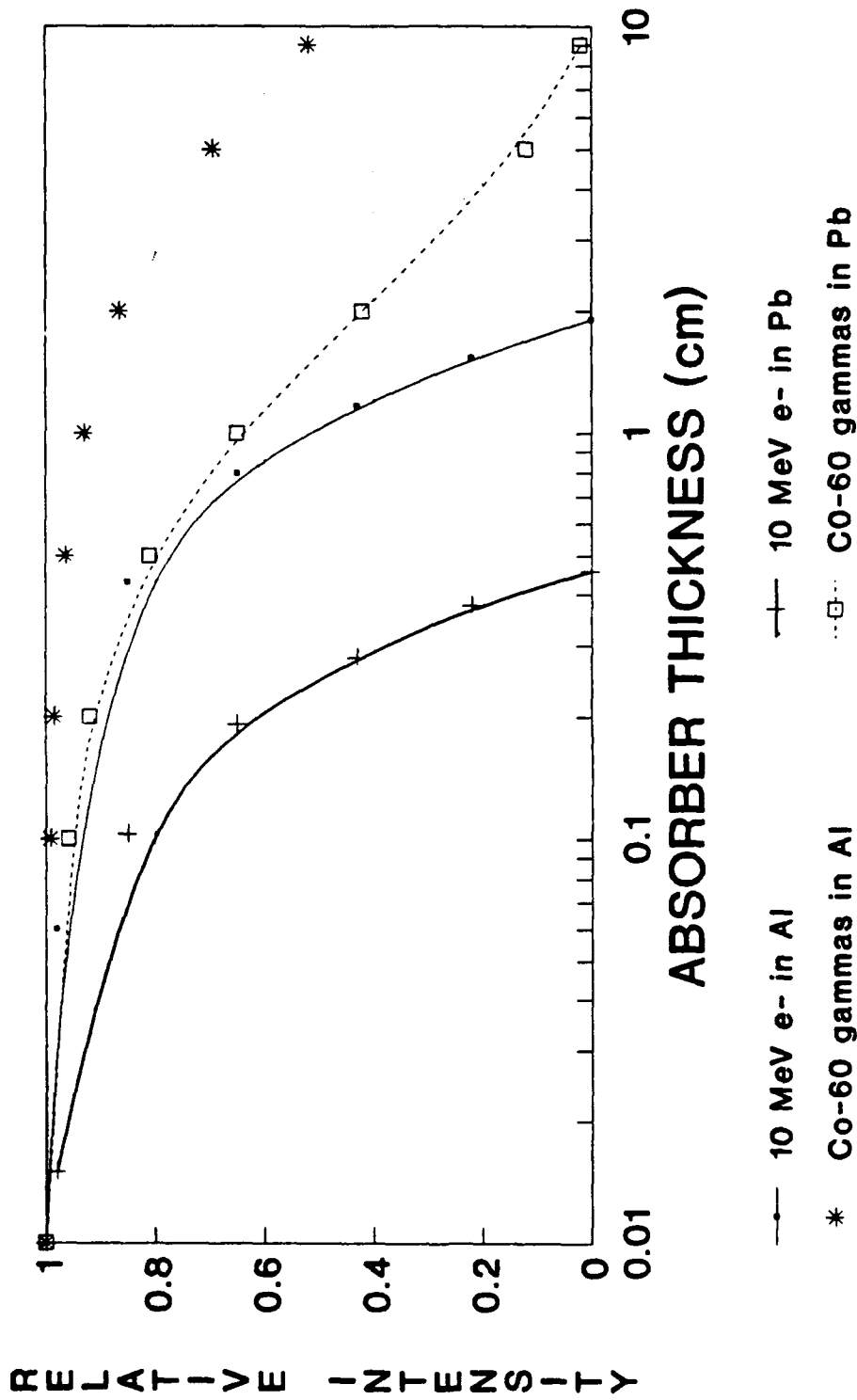


Figure 4: Comparison of attenuation of 10 MeV electrons and ⁶⁰Co Gamma-rays in Pb and Al.

■ E Plane: ERR Zoom Level: 1/2X
 ACTIVE Data Bit: d0
Err Ctr: 3871
D Plane: OUTPUT Origin: 0, 0
Err Ctr: 131657 Size: 200,200
 Cursor: ---

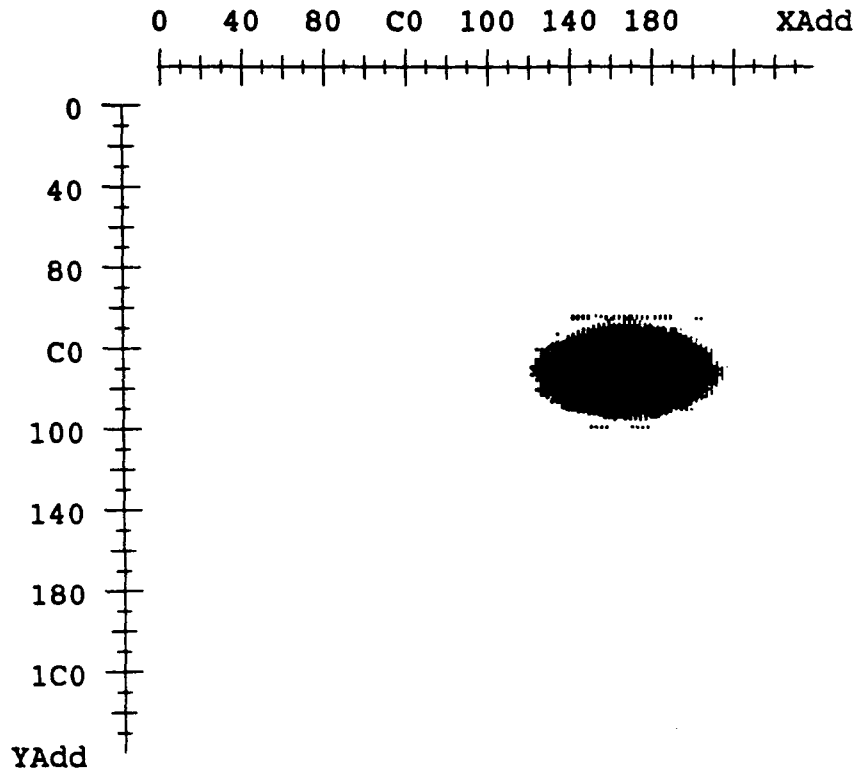


Figure 5: FCR display showing the transmission pattern of 8 MeV electrons through 1/32" collimator onto NEC DRAM. Note the central pattern caused by direct ionization, and the photocurrent effects along the x and y decoder lines.

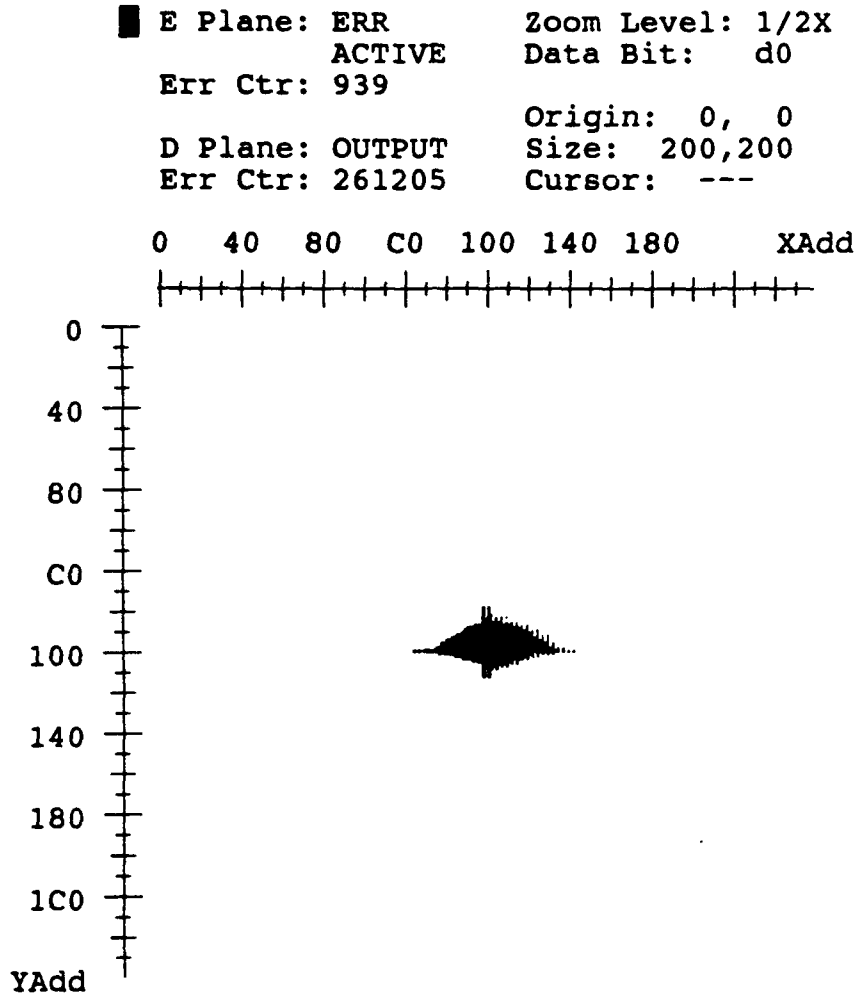


Figure 6: FCR display showing transmission pattern of 8 MeV electrons through 1/32" collimator onto the NEC DRAM, aimed directly at the chip centre (intersection of x and y decoder lines). The transmission along the decoder lines masks the collimator image.

■ E Plane: ERR Zoom Level: 1/2X
 ACTIVE Data Bit: d0
 Err Ctr: 12800

 D Plane: OUTPUT Origin: 0, 0
 Err Ctr: 131972 Size: 200,200
 Cursor: ---

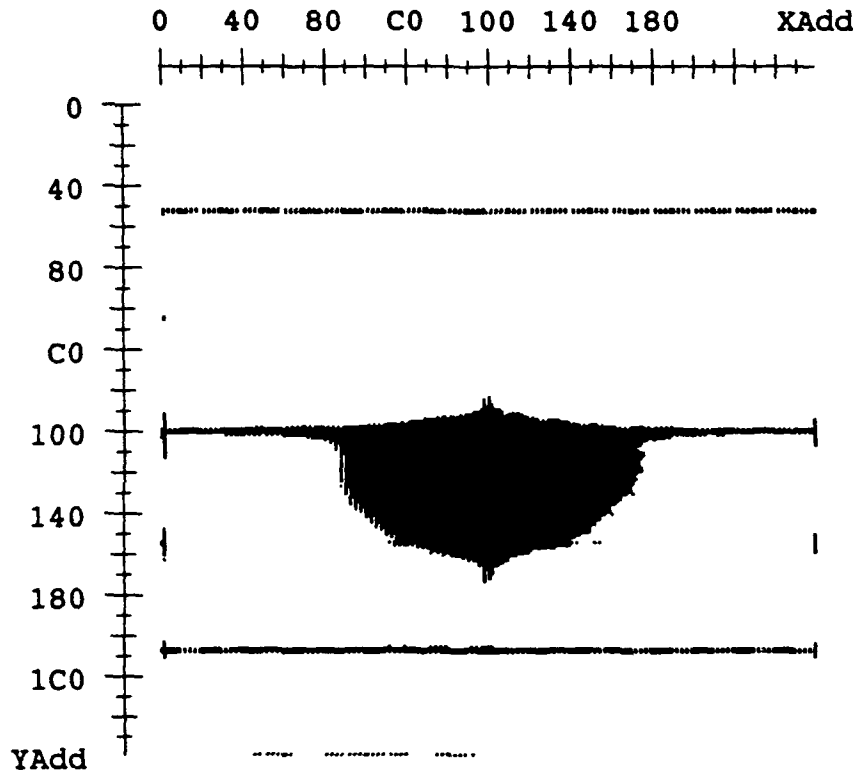


Figure 7: The same experimental set up as in fig 6, but at a higher dose rate. Note that spreading and decoder line effects render recognition of the direct collimator image impossible.

```

■ E Plane: ERR      Zoom Level: 2X
      ACTIVE      Data Bit:  d0
Err Ctr: 242

D Plane: OUTPUT    Origin:  0,  0
Err Ctr: 242      Size:    80, 80
                  Cursor:  ---

```

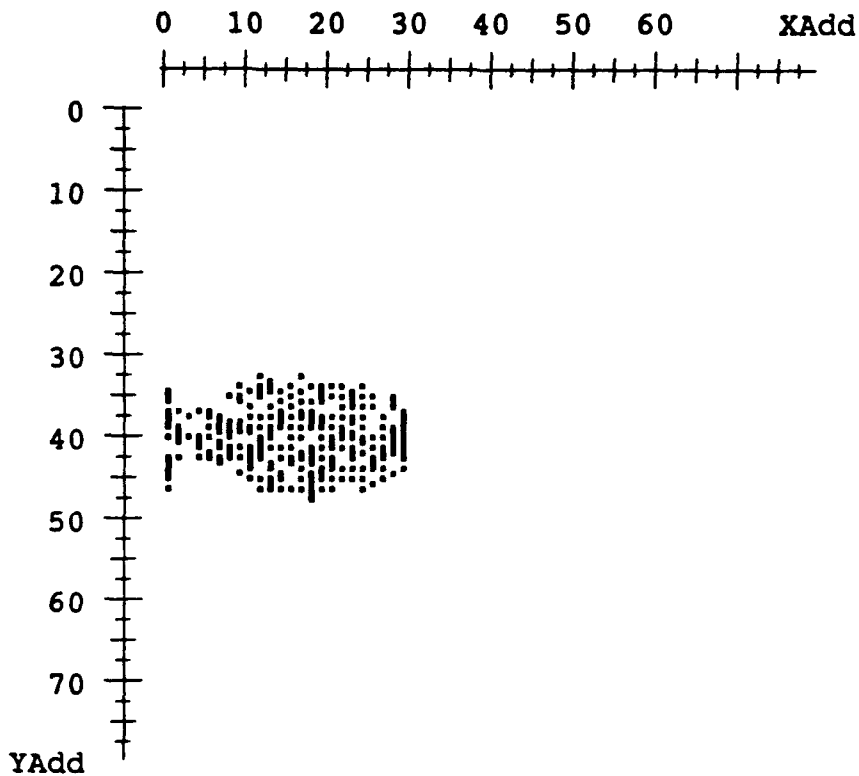


Figure 8(a): FCR display showing transmission pattern of 8 MeV electrons through 1/32" collimator onto the AMD SRAM, with all bits originally set to '0'. Note the elliptical image due to cell aspect ratio.

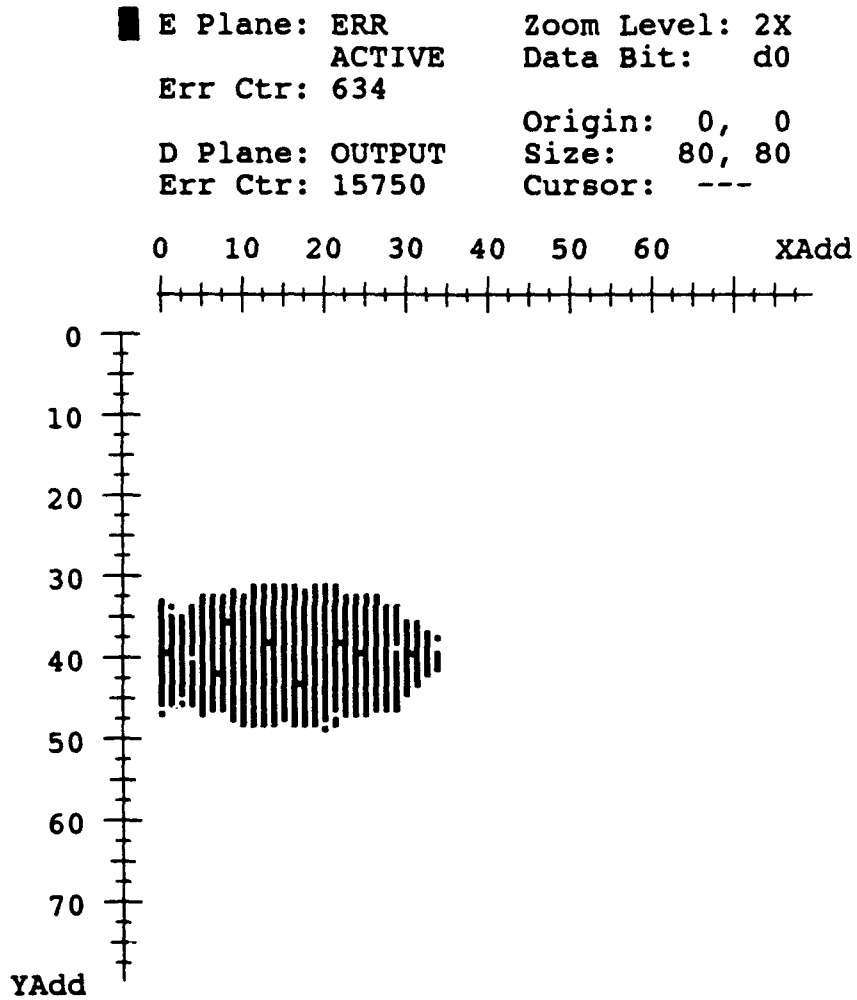


Figure 8(b): FCR display showing transmission pattern of 8 MeV electrons through 1/32" collimator onto the AMD SRAM, with all bits originally set to '1'. Clearly this setting is more sensitive than the '0' case.

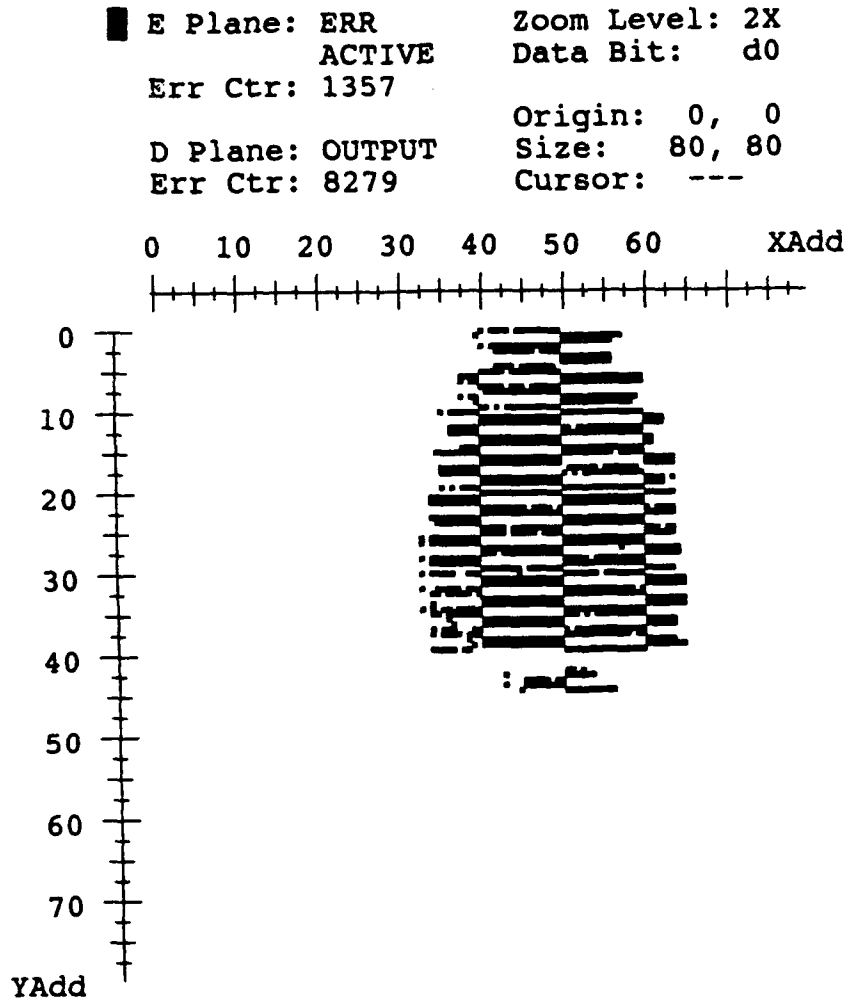


Figure 9: Same experimental set-up as in fig 8(b), but with much higher dose rate and with collimator physically moved. Note that although the elliptical pattern grows, it is still recognizable.

```

■ E Plane: ERR      Zoom Level: 2X
                ACTIVE   Data Bit:  d0
Err Ctr: 1408
                Origin:  0,  0
D Plane: OUTPUT    Size:   80, 80
Err Ctr: 14976    Cursor:  ---

```

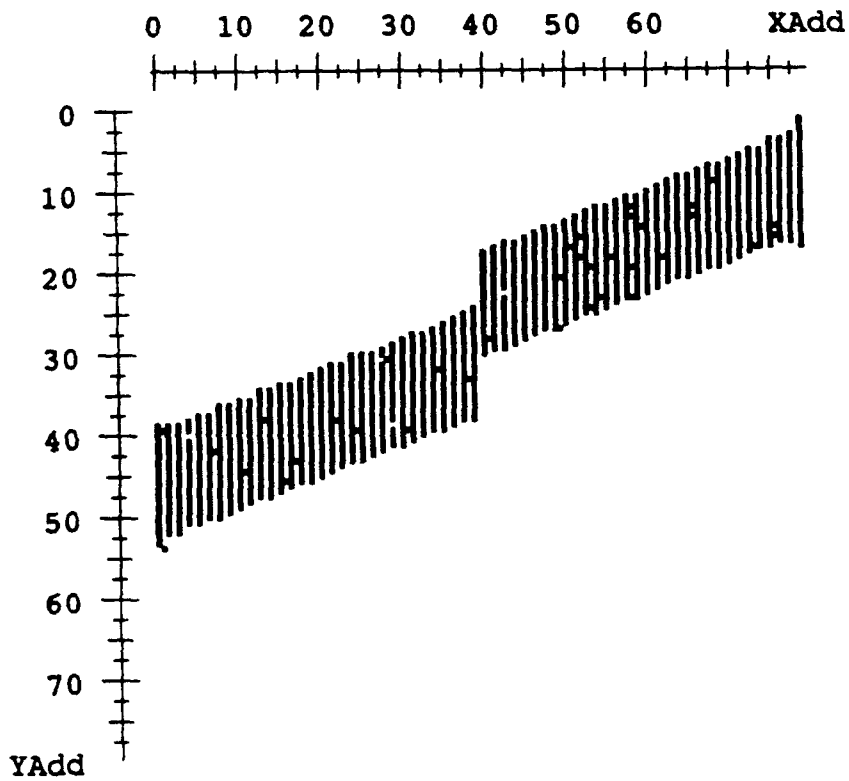


Figure 10: FCR display showing the transmission pattern of 8 MeV electrons through a $(.018 \pm .003)$ inch wide slit arranged diagonally across the AMD SRAM chip. The discontinuity is due to the chip decoder strip.

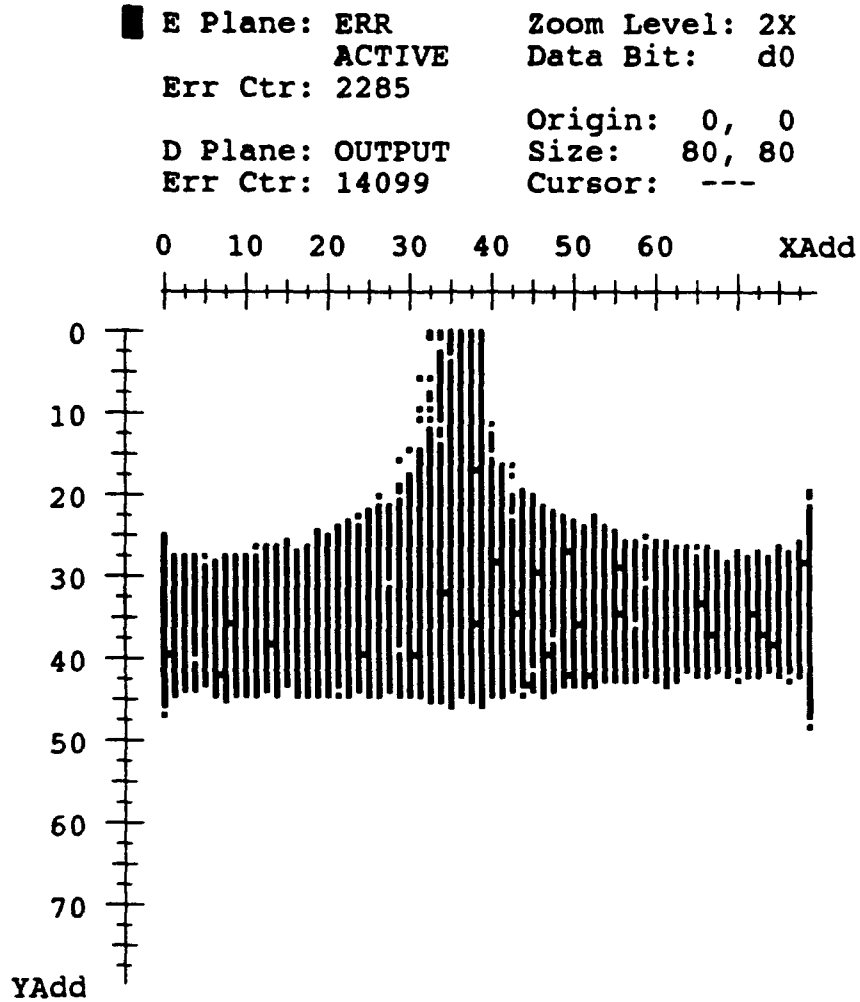


Figure 11: FCR display showing the transmission pattern of 8 MeV electrons through an "inverted T" (formed by the intersection of three Al plates) onto the AMD SRAM.

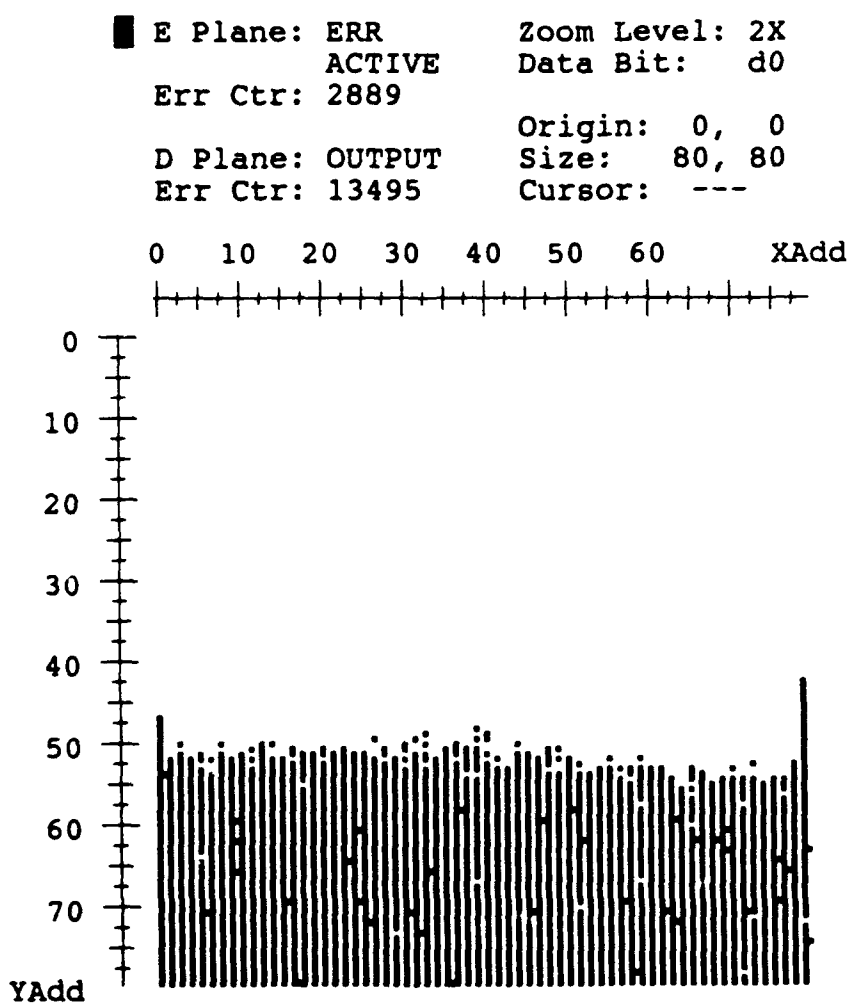


Figure 12: FCR display showing the transmission pattern on the AMD SRAM arising from an Al plate shadowing the upper half of the chip.

```

■ E Plane: ERR          Zoom Level: 2X
                ACTIVE      Data Bit:  d0
Err Ctr: 1728

D Plane: OUTPUT      Origin:  0,  0
Err Ctr: 14656      Size:    80, 80
                Cursor:  ---

```

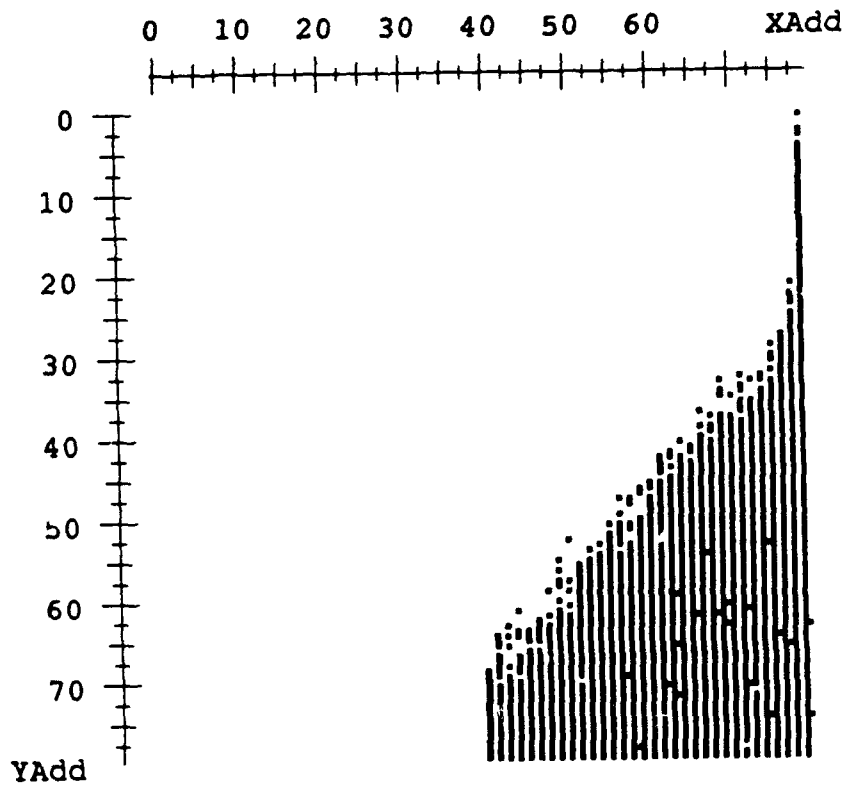


Figure 13: FCR display showing the transmission pattern on the AMD SRAM arising from an Al plate placed diagonally across the chip. Note that decoder strip and some edge effects are apparent.

■ E Plane: ERR Zoom Level: 2X
 ACTIVE Data Bit: d0
Err Ctr: 4062
D Plane: OUTPUT Origin: 0, 0
Err Ctr: 12322 Size: 80, 80
 Cursor: ---

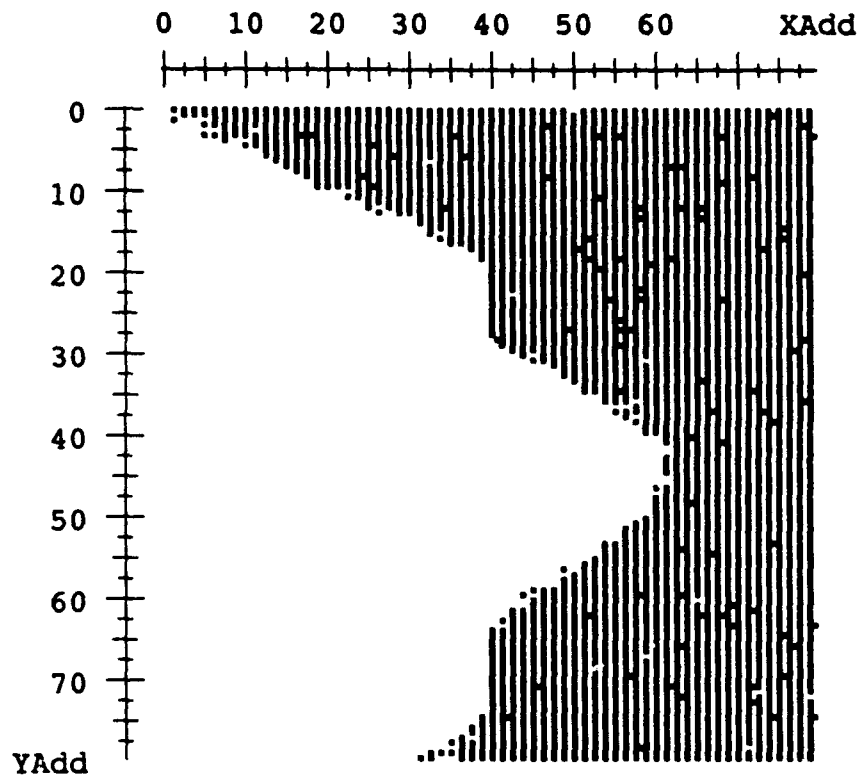


Figure 14: FCR display showing the transmission pattern on the AMD SRAM arising from a corner of the Al plate intersecting the beam. The decoder strip effect are apparent.

6.0 REFERENCES

1. Anisimov, Y.S. et al "Development and Investigation of a Neutron Radiography Imaging System with a Low-Pressure Multistep Chamber Nuclear Inst. Meth., vol; A273, no 2-3 , 1988
2. Briggs, C.W. "Developments in Gamma-Ray Radiography 1928 to 1941" presented at American Industrial Radium and X-Ray Society Meeting, Cambridge. MA. 1941.
3. Jacobs, A.M., J.D. Cox and Y.S. Juang, "The DRAM as an X-Ray Sensor" Proceedings of Int. Soc. Opt. Eng., vol 767, part 1, 1987.
4. Cousins, T. and E.L. Karam, "An Examination of Radiation-Induced Bit-Upset Patterns in Semiconductor Memories" DREO Report, To be published.
5. Semiconductor Insights Inc., proprietary disclosure to DREO.
6. MacGillivray, G.M., Chalk River Nuclear Laboratories. Personal Communication to DREO.
7. Messenger, G.G. and M.S. Ash "The Effects of Radiation on Electronic Systems" Van Nostrand Reinhold Co., New York, 1986.
8. Marshall, J. and A.G. Ward, Can. J. Research AIS, 1937.
9. Siegbahn, K., "Alpha-, Beta- and Gamma-Ray Spectroscopy" Vol 1, North Holland Publishing Company, Amsterdam, 1965.
10. Brodksy, A.B. "CRC Handbook of Radiation Measurement and Protection" CRC Press. West Palm Beach, Fla., 1978.
11. Pickel, J.C. and J.T. Blandford, "Cosmic Ray Induced Errors in MOS RAMs", IEEE Trans. Nuc. Sci., NS-27 (2), Apr. 1980.
12. Cousins, T. and K.M. Qureshi, "Transient Annealing Characteristics of Irradiated MOSFETs" DREO Report, To be published.

SECURITY CLASSIFICATION OF FORM
(highest classification of Title, Abstract, Keywords)

DOCUMENT CONTROL DATA

(Security classification of title, body of abstract and indexing annotation must be entered when the overall document is classified)

<p>1. ORIGINATOR (the name and address of the organization preparing the document. Organizations for whom the document was prepared, e.g. Establishment sponsoring a contractor's report, or tasking agency, are entered in section 8.) Defence Research Establishment Ottawa, Ontario KIA 0Z4</p>		<p>2. SECURITY CLASSIFICATION (overall security classification of the document, including special warning terms if applicable) UNCLASSIFIED</p>	
<p>3. TITLE (the complete document title as indicated on the title page. Its classification should be indicated by the appropriate abbreviation (S,C or U) in parentheses after the title.) MICRO-RADIOGRAPHY USING AN ELECTRON LINAC SOURCE AND RAM MEMORY CHIP DETECTORS (U)</p>			
<p>4. AUTHORS (Last name, first name, middle initial) Cousins, T., Karam, E.L., and Brisson, J.R.</p>			
<p>5. DATE OF PUBLICATION (month and year of publication of document) June 1990</p>	<p>6a. NO. OF PAGES (total containing information. Include Annexes, Appendices, etc.) 29</p>	<p>6b. NO. OF REFS (total cited in document) 12</p>	
<p>7. DESCRIPTIVE NOTES (the category of the document, e.g. technical report, technical note or memorandum. If appropriate, enter the type of report, e.g. interim, progress, summary, annual or final. Give the inclusive dates when a specific reporting period is covered.) DREO Technical Report</p>			
<p>8. SPONSORING ACTIVITY (the name of the department project office or laboratory sponsoring the research and development. Include the address.) Defence Research Establishment Ottawa Ottawa, Ontario KIA 0Z4</p>			
<p>9a. PROJECT OR GRANT NO. (if appropriate, the applicable research and development project or grant number under which the document was written. Please specify whether project or grant) 041LS</p>	<p>9b. CONTRACT NO. (if appropriate, the applicable number under which the document was written)</p>		
<p>10a. ORIGINATOR'S DOCUMENT NUMBER (the official document number by which the document is identified by the originating activity. This number must be unique to this document.) DREO Technical Note 90-16</p>	<p>10b. OTHER DOCUMENT NOS. (Any other numbers which may be assigned this document either by the originator or by the sponsor)</p>		
<p>11. DOCUMENT AVAILABILITY (any limitations on further dissemination of the document, other than those imposed by security classification) <input checked="" type="checkbox"/> (X) Unlimited distribution <input type="checkbox"/> () Distribution limited to defence departments and defence contractors; further distribution only as approved <input type="checkbox"/> () Distribution limited to defence departments and Canadian defence contractors; further distribution only as approved <input type="checkbox"/> () Distribution limited to government departments and agencies; further distribution only as approved <input type="checkbox"/> () Distribution limited to defence departments; further distribution only as approved <input type="checkbox"/> () Other (please specify):</p>			
<p>12. DOCUMENT ANNOUNCEMENT (any limitation to the bibliographic announcement of this document. This will normally correspond to the Document Availability (11). However, where further distribution (beyond the audience specified in 11) is possible, a wider announcement audience may be selected.)</p>			

13. ABSTRACT (a brief and factual summary of the document. It may also appear elsewhere in the body of the document itself. It is highly desirable that the abstract of classified documents be unclassified. Each paragraph of the abstract shall begin with an indication of the security classification of the information in the paragraph (unless the document itself is unclassified) represented as (S), (C), or (U). It is not necessary to include here abstracts in both official languages unless the text is bilingual).

Radiography using a pulsed electron (LINAC) source and a semiconductor memory chip (RAM) as a detector has been investigated. The responses of commercial SRAMS and DRAMS were examined, with the SRAM proving superior for radiography. A variety of shapes (circular holes, slits, etc.) were radiographed with the results being encouraging for future work.

14. KEYWORDS, DESCRIPTORS or IDENTIFIERS (technically meaningful terms or short phrases that characterize a document and could be helpful in cataloguing the document. They should be selected so that no security classification is required. Identifiers, such as equipment model designation, trade name, military project code name, geographic location may also be included. If possible keywords should be selected from a published thesaurus. e.g. Thesaurus of Engineering and Scientific Terms (TEST) and that thesaurus-identified. If it is not possible to select indexing terms which are Unclassified, the classification of each should be indicated as with the title.)

Electron Linear Accelerator (LINAC)
Radiography
RAM
Semiconductor Memories
Gamma Ray
Bit-Map
Bremsstrahlung